AIAA JOURNAL
Vol. 40, No. 1, January 2002

# Transducer for Direct Measurement of Skin Friction in Hypervelocity Impulse Facilities

C. P. Goyne,* R. J. Stalker,† and A. Paull‡
*University of Queensland, Brisbane, Queensland 4072, Australia*

**An acceleration compensated transducer was developed to enable the direct measurement of skin friction in hypervelocity impulse facilities. The gauge incorporated a measurement and acceleration element that employed direct shear of a piezoelectric ceramic. The design integrated techniques to maximize rise time and shear response while minimizing the affects of acceleration, pressure, heat transfer, and electrical interference. The arrangement resulted in a transducer natural frequency near 40 kHz. The transducer was calibrated for shear and acceleration in separate bench tests and was calibrated for pressure within an impulse facility. Uncertainty analyses identified only small experimental errors in the shear and acceleration calibration techniques. Although significant errors were revealed in the method of pressure calibration, total skin-friction measurement errors as low as ± 7–12% were established. The transducer was successfully utilized in a shock tunnel, and sample measurements are presented for flow conditions that simulate a flight Mach number near 8.**

## Nomenclature

| | | |
|---|---|---|
| $b$ | = | pressure calibration constant (slope), V/kPa |
| $C_f$ | = | local skin-friction coefficient, $\tau_w/\frac{1}{2}\rho U^2$ |
| $c$ | = | acceleration calibration constant |
| $D$ | = | diameter of skin-friction transducer sensing disk, m |
| $d$ | = | shear calibration constant (slope), V/Pa |
| $e$ | = | pressure calibration constant (voltage axis intercept), V |
| $g$ | = | acceleration due to gravity, m/s$^2$ |
| $h$ | = | enthalpy, MJ/kg |
| $J$ | = | moment, N · m |
| $M$ | = | mainstream Mach number |
| $m$ | = | mass, kg |
| $P$ | = | static pressure, kPa |
| $Re_x$ | = | Reynolds number, $\rho U x/\mu$ |
| $U$ | = | mainstream velocity, m/s |
| $u$, $v$ | = | Cartesian velocity components |
| $V$ | = | voltage, V |
| $x$ | = | Cartesian coordinate and distance from leading edge, m |
| $y$ | = | Cartesian coordinate |
| $z$ | = | length of moment arm, m |
| $\theta$ | = | angle in shear calibration technique |
| $\mu$ | = | mainstream viscosity, Ns/m$^2$ |
| $\rho$ | = | mainstream density, kg/m$^3$ |
| $\tau$ | = | boundary-layer shear stress, Pa |

*Subscripts*

| | | |
|---|---|---|
| $a$ | = | acceleration component |
| $P$ | = | pressure component |
| $s$ | = | stagnation |
| sf | = | skin-friction component |
| $w$ | = | wall |
| 0 | = | zero-deg orientation |
| 1 | = | measuring piezoelectric element |
| 2 | = | acceleration compensating piezoelectric element |
| 180 | = | 180-deg orientation |

Received 8 May 2000; revision received 16 February 2001; accepted for publication 13 June 2001. 

*Postgraduate Scholar, Department of Mechanical Engineering; currently Research Associate, Department of Mechanical and Aerospace Engineering, University of Virginia, Charlottesville, VA 22904. Member AIAA.

†Emeritus Professor, Department of Mechanical Engineering. Associate Fellow AIAA.

‡Senior Research Fellow, Department of Mechanical Engineering.

## Introduction

SKIN-FRICTION drag is expected to limit significantly the performance of vehicles designed for sustained hypersonic flight. For example, estimates indicate that skin friction can contribute around one-third of the total drag of propulsive devices such as scramjet engines.[1] On vehicle surfaces, the skin-friction component can be expected to be even higher. If one considers a flat plate at incidence at Mach 16, for example, and assumes a turbulent boundary layer with a skin-friction coefficient of $1.7 \times 10^{-3}$, then it is readily shown that the inviscid drag is equal to the viscous drag when the angle of attack is 7 deg. This angle of surface incidence is of the same order as can be expected for sustained hypersonic flight. Thus, considering the vehicle and propulsive device, it is clear that the total skin-friction drag will be a major component of the overall vehicle drag. Although the skin-friction component is expected to be significant, actual levels are difficult to predict accurately, and this is largely due to the challenges of directly measuring skin friction in hypervelocity facilities.

Hypervelocity impulse facilities, such as shock tunnels and expansion tubes, provide the only practical means of producing the high-Mach-number and high-stagnation-enthalpy flows that correctly simulate hypersonic flight. Test times in these facilities, however, are extremely short. For example, test time lengths for shock tunnels and expansion tubes capable of scramjet testing are typically a few milliseconds and a few hundreds of microseconds, respectively. Hence, skin-friction instrumentation must have an appropriately fast response to shear loads. The transient nature and high levels of heat transfer, pressure, and acceleration in the test section exacerbate this requirement. Such factors have contributed to a lack of accurate skin-friction instrumentation for hypervelocity impulse facility testing. This has resulted in a lack of data for high-enthapy flows, and hence, considerable uncertainty exists in relation to theoretical skin-friction prediction methods.

A skin-friction transducer is only suitable for use in an impulse facility if its response time is short. Transducers with short response times inherently have light stiff components with little internal damping. This results in a highly resonant gauge that has multiple natural frequencies and has a gain that varies with input frequency. According to Wright,[2] such transducers can be used to make valid waveshape measurements up to 25% of the first natural frequency. Up to this point, the amplitude response will vary by a maximum of 5%, and the phase response will be approximately linear. Thus, a skin-friction transducer with high natural frequencies will allow a more accurate reproduction of a high-frequency skin-friction waveshape. The importance of high natural frequencies for an impulse

flow skin-friction transducer can also be demonstrated by considering the length of steady test time available from the facility or the length of a particular event of interest during a test. At least five cycles of the lowest natural frequency is generally regarded as a conservative estimate if mean level information is to be obtained from a signal.[3,4] For example, if the available test time is half a millisecond, then a lowest natural frequency of at least 10 kHz would reasonably be required. If skin-friction fluctuations with a period of, say, one-fifth of this test time are to be resolved accurately, then the requirement of Wright[2] would dictate a lowest natural frequency of at least 40 kHz. Although this choice is somewhat arbitrary, experience has shown that a skin-friction transducer with a lowest natural frequency near 40 kHz is suitable for resolving fluctuations resulting from unsteady processes such as combustion[5] or boundary-layer transition.[6]

High-frequency transducers that directly measure skin friction have been used in hypervelocity impulse facilities since the late 1960s. Four different transducers have been developed for the task, with mixed success. Wallace[7] and Holden[8] reported early use of a skin-friction transducer in shock tunnels. The transducer consisted of two piezoelectric cantilever beams supporting a floating element flush with the model surface. A third cantilever with a mass attached, but not exposed to the flow, allowed for acceleration compensation. The arrangement resulted in a natural frequency of approximately 5 kHz (Ref. 9), which in the current context is relatively low.

Jessen et al.[10] described a skin-friction transducer that consisted of a 4-mm-diam floating element attached to a cantilever beam. Two semiconductor strain gauges measured the deflection of the beam in two orthogonal components, and this enabled the two-component measurement of skin friction. The design resulted in a natural frequency near 10 kHz, and the gauge was applied to a shock tunnel. The authors reported that difficulties were encountered and were not fully resolved. Thermal loads resulted in strain gauge drift, and vibration affected the gauge output.

Bowersox et al.[11] reported on a skin-friction transducer that was also applied to shock-tunnel experiments. The gauge consisted of a plastic cantilever that was presented to the flow with a 4.6-mm-diam floating element head. Two strain gauges were mounted near the base of the cantilever, and the signals were combined to cancel pressure sensitivity. In an attempt to limit pressure gradient, heat transfer, and vibration effects, the cavity surrounding the cantilever was filled with silicon oil. The design resulted in a natural frequency of 10 kHz. Novean et al.[12] later modified the gauge to achieve a natural frequency of 20 kHz, and the transducer was used in an expansion tube. Encouraging results were obtained. However, the potential for oil leakage from the sensing cavity raised concerns of oil replenishment requirements and of contamination of other instrumentation. In some tests, silicon rubber was used in place of the silicon oil; however, this was found to reduce shear sensitivity and increase the effects of vibration and pressure gradients. For the present study, the presence of oil or rubber in the gap surrounding the floating element of the skin-friction transducer was, therefore, regarded as detrimental to transducer operability and performance. It may be argued that the unfilled gap will lead to measurement errors when the transducer is operated in a flow with a pressure gradient; however, as outlined by Winter,[13] appropriate gauge design can limit the induced errors to the point that they are one to two orders of magnitude lower than skin-friction levels.

To achieve higher natural frequencies than obtained with cantilever-type transducers, Kelly et al.[14] developed a skin-friction transducer that employed direct shear of a piezoelectric element. The gauge was applied to shock tunnels. The design consisted of a floating element sensing disk that was directly adhered to a series of piezoceramics. Early designs resulted in natural frequencies above 300 kHz, although later modifications[15] reduced natural frequencies to the range of 40–60 kHz. Unfortunately, an acceptable shear calibration technique, independent of the shock-tunnel test flow, was not established. This resulted in the need to infer a calibration for the transducer from other measured test flow parameters. The gauge was also severely affected by vibration of the test model.

This paper reports on a new skin-friction transducer that has resulted from further modification and development of the gauge due to Kelly et al.[14] and Kelly.[15] The new transducer incorporates features to minimize the effects of acceleration, pressure, heat transfer, and electrical interference, while maximizing shear response and maintaining a relatively high first natural frequency, of approximately 40 kHz. The gauge is manufactured at the University of Queensland and has been applied to laminar, transitional, and turbulent boundary layers in a shock tunnel[6] and to supersonic combustion experiments in a shock tunnel.[5] The stagnation enthalpy of the test flows simulated flight Mach numbers in the range of 8–21. The paper begins by describing the design and calibration of the new gauge. Particular attention is paid to the experimental uncertainties inherent in the calibration and measurement techniques. Some sample experimental results are then highlighted before the conclusion.

## Design

### A. Piezoelectric Effect

The piezoelectric effect is a most appropriate method for sensing shear in a hypervelocity impulse facility. Piezoelectric elements are inherently stiff and result in high transducer natural frequencies with minimum deflection under load. More important, the shear response of such elements can be effectively decoupled from other forces such as tension, compression, and transverse shear. Piezoelectric transducers also typically have a large dynamic range and exhibit very little hysteresis.[2]

Jaffe et al.[16] define piezoelectricity as the ability of a certain crystalline material to develop an electrical charge that is proportional to a mechanical stress. Conversely, the material changes shape when an electric field is applied. The piezoelectric material used for the present transducer is lead zirconate titanate ceramic (PZT), and as with all piezoelectric materials, PZT is highly anisotropic. From crystallographic considerations, it can be shown that PZT will produce a charge on electroded surfaces that is linearly proportional to an applied shear force. Furthermore, the charge output is not a function of tension, compression, hydrostatic forces (pressure), or orthogonal shear forces.[6,15,16] This is provided that the material is operated in a fashion referred to as shear mode. Here the electrodes are located on a pair of parallel surfaces that are on a plane parallel to the poling axis of the material. Thus, a skin-friction gauge incorporating PZT operated in shear mode should have a defined axis of maximum sensitivity to shear and zero sensitivity to pressure and cross axis shear. However, manufacturing deficiencies introduce some sensitivity to pressure and cross axis shear, and as discussed later, calibration techniques can be used to quantify these effects.

### B. Transducer

The gauge of the present study is schematically detailed in Fig. 1. The layout consisted of a measuring element that was exposed to the flow and an acceleration compensating element that was located within the gauge housing. The measuring element was simultaneously subjected to shear, pressure, heat transfer, and acceleration, while the compensating element, protected from the flow, experienced only acceleration forces. Each element incorporated one ring of PZT piezoceramic operated in shear mode. The use of one ring

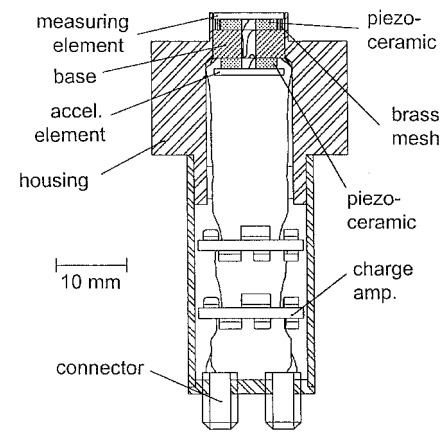


**Fig. 1 Schematic of skin-friction transducer.**

in each element, rather than multiple rings, limited the transducer to the measurement of one component of skin friction.

The piezoceramic rings were 1.5 mm in thickness, and the outer diameter was 8 mm. A 2-mm inner diameter allowed the routing of electrode contact leads. The poling axis of the piezoceramic defined the measurement axis of the transducer, and the flat faces of the ring, parallel to the pole axis, were electroded with silver paint. The measuring piezoceramic was protected from the flow by a 10-mm-diam, 0.81-mm-thick disk of the low expansion alloy invar. The invar disk was mounted flush with the model surface and formed the shear sensing surface of the gauge. The disk dimensions and material were similar to those chosen by Kelly et al.[14] and Kelly.[15] Coatings of acrylic and polyurethane insulation and electrically conductive paint protected the sides of both ceramics (the conductive paint was applied over the acrylic and polyurethane and, hence, was electrically insulated from the piezoceramics). The sensing ceramic was also wrapped in approximately 11 layers of fine brass mesh. This acted to cool the freestream air that entered the cavity formed between the piezoceramic–invar assembly and the brass housing. Significant quantities of freestream air were expected to enter the cavity only up to the point of 20–50 $\mu$s after arrival of the test flow. This was determined by treating the invar-housing gap as a sonic throat that vented into the known volume of the transducer cavity. Thermal analyses indicated that the combination of invar, insulation coatings, and mesh were able to effect adequate thermal protection of the measuring piezoceramic for boundary-layer heat transfer loads of up to 7.5 MW/m$^2$ for a period of at least 3 ms (Ref. 6).

The sensing invar disk and the gauge housing formed a clearance gap of $0.16 \pm 0.01$ mm. Maximum displacement of the measuring element at the sensing disk was estimated to be $5 \times 10^{-7}$ mm. This was based on the total of bending and shear deflection of a PZT element for a 3000-Pa skin-friction load on the sensing disk.

Each piezoceramic was adhered to an aluminum base, which was in turn located within the brass housing of the gauge. Component size and weight were minimized, and stiffness was maximized to maximize resonant frequencies of the piezoceramic assembly. As discussed later, the arrangement resulted in a first natural frequency of approximately 40 kHz.

To simulate the acceleration response of the measuring element, the acceleration element was mounted within the gauge in a manner identical to the measuring element. Thus, the acceleration piezoceramic was also operated in shear mode, with the poling axis aligned along the same axis as that of the measuring element. Both ceramics were of the same dimensions and were coated with insulation and fastened to an invar disk in the same manner. Brass mesh, however, was not applied around the acceleration element; subsequent calibration revealed that this did not degrade the accuracy of the acceleration compensation method. Because the ceramics were operated in shear mode, both elements were nominally only sensitive to acceleration along the measuring axis. By monitoring the output of the acceleration element and the measuring element during service, the gauge could be compensated for acceleration by subtraction of one signal from the other.

Two purpose-built charge amplifiers were located within the gauge housing, and each amplifier was connected to one ceramic. When powered by a constant current power supply, these amplifiers produced a change in voltage that was proportional to the change in charge on the piezoceramic electrodes. The amplifiers had a rise time near 2 $\mu$s and a decay time constant of 47 ms. All metallic components of the gauge, including the electrically conductive paint surrounding the piezoceramics, were adequately earthed via coaxial connectors on the rear of the gauge housing. This resulted in an electrical shield that fully enclosed the piezoceramics, electrodes, internal leads, and charge amplifiers. Hence, these components were protected from background electromagnetic fields and any effects of ionization of the impulse facility test gas.

### C. Mounting System

The mounting system was designed to maximize vibration and acceleration isolation of the skin-friction transducer while adequately locating the gauge and preventing test flow leakage. As shown in Fig. 2, a felt isolator system was adopted for the present transducer. Felt is a popular choice for high-frequency applications because of high internal damping and a mechanical impedance that is dissimilar to that of many engineering materials.[17] (Hence, transmissibility of a felt to metal interface, for example, is low.) For the present system, felt washers were used on the front and back faces of the transducer main housing, and a smaller washer was mounted at the rear of the electronics housing. The two main housing washers located the gauge axially, and the rear washer aided location of the gauge within the center of the tapping hole in the model. The use of paper shims and a threaded brass mounting sleeve enabled compensation for felt compression due to aging. This allowed flushness of the sensing face with the model surface to be maintained; however, the arrangement resulted in the need to adjust the mount before every run in the impulse facility. The mount could be operated with the gauge mounted face down or face up, that is, mounted in the lower or upper wall of a duct, etc.

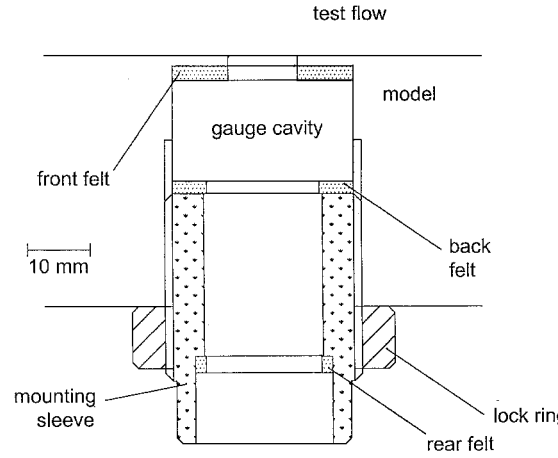


**Fig. 2 Schematic of skin-friction transducer mount.**

Applied shear and pressure forces were expected to displace the transducer during the test time, and hence, appropriate amounts of mass were incorporated into the gauge housing to limit the effect. Based on the expected stiffness of the felt washers and a 3-ms-duration step input of shear and pressure on the sensing face of the gauge, calculations indicated that transducer displacement would not be significant. A 3000-Pa skin-friction load on the sensing face was expected to produce only 13-$\mu$m translation in the flow direction and 0.08-deg rotation about the center of mass. For static pressures in the range of 10–100 kPa, maximum axial translation away from the test flow was expected to be near 50 $\mu$m.

Because of the porosity of the felt washers, a finite amount of test gas was expected to leak through the skin-friction gauge mount. As a result of a lack of compressible flow data on felt leakage, a simple experiment was devised to measure the amount of leakage through the gauge mount. A skin-friction transducer was mounted in a cast iron calibration block, using the mount of Fig. 2, and a pressure differential was applied across the mount and gauge using a pressure calibration rig.[15] The apparatus enabled a known pressure to be applied to the test flow side of the skin-friction gauge and model. The pressure and temperature at the rear of the mount remained at ambient room values. The velocity of air issuing from the rear of the mount was measured using a commercial air velocity meter. The point of measurement was at the exit of the gap formed between the skin-friction gauge and mounting sleeve. From knowledge of the air velocity, the dimensions of the gap and assuming ambient room density of the exiting gas, the mass flow rate of air leakage was established to be $(1 \pm 0.2) \times 10^{-4}$ and $(15 \pm 3) \times 10^{-4}$ kg/s for a pressure differential of 10 and 100 kPa, respectively.

To quantify the effect of these leakage levels on the instrumented boundary layer of an experiment, estimates were made of the mass flux in the boundary layer that were expected to pass over the transducer for a typical application.[6] The experimentally determined leakage levels were found to be of the order of a few percent of the boundary-layer mass flux. Effects of such leakage can be regarded

as negligible when it is considered that actual test flow leakage will involve gas that is supplied by a high-enthalpy boundary layer. Gas temperatures in the vicinity of gauge to test model gap would be expected to be 2–6 times greater than that of the devised test. Hence, actual leakage mass flow rates will be very low because of low flow density and high viscosity.

Although the leakage rates are expected to be low, White[18] shows that even small amounts of boundary-layer leakage, or suction, can affect the local skin friction. To experimentally assess the effect of mount leakage on measured skin-friction levels, tests were conducted in the T4 shock tunnel in which the felt mounting washers were replaced with impervious rubber O-rings. The measurements were conducted during testing of an early prototype skin-friction gauge and were obtained on a flat plate in air ($Re_x = 2 \times 10^6$, $M = 6$, and $h_s = 3.6$ MJ/kg). Rubber O-rings were found to increase vibration and acceleration transmission to the skin-friction gauge and shorten the duration of useful signal from the transducer. However, up to 0.2 ms after the onset of the test flow, the skin-friction gauge was capable of functioning adequately while mounted using O-rings. When the transducer was mounted using rubber O-rings, the measured level of skin friction during the 0.2-ms period was the same as when mounted using felt washers. The tests, therefore, demonstrated that in the developing boundary layer of the test flow, the measured level of skin friction was the same with and without a small amount of leakage into the skin-friction gauge mount.

Such a limited effect of mount leakage can be expected when the boundary-layer momentum equation is considered for the case of localized suction. If the normal velocity of flow at the wall, $v_w$, is finite and there is no pressure gradient in the flow, then the momentum equation dictates that $\partial\tau/\partial y$ is finite very close to the wall.[18] Hence, at the point of leakage to the felt mount, $v_w < 0$, and the distribution of $\tau$, and hence $\tau_w$, is affected. However, referring to Figs. 1 and 2 it is noted that the point of leakage is through the gap between the gauge housing and model, an area that is removed from the shear sensing surface of the skin-friction gauge. At the sensing surface itself there is no leakage, and $v_w = 0$; thus, $\partial\tau/\partial y$ is zero, and the skin friction remains unaltered. On the model test surface, $v_w$ is also zero, and $\partial\tau/\partial y$ is zero. Noting that $\partial\tau/\partial x$ is low, if a small amount of leakage occurs, then a thin layer of fluid approaching the skin-friction gauge is removed, and one constant shear layer is replaced by another in which the shear stress, and hence $\tau_w$, has the same value. Given that the same level of skin friction was measured in a developing boundary layer with and without mount leakage, the shear layer disturbance would appear to have no downstream effect on the level of skin friction encountered by the sensing surface of the gauge.

## Calibration

The skin-friction transducer was calibrated for shear and acceleration in separate bench tests. Natural frequencies of the gauge and sensitivity to moments on the sensing face were also explored in bench tests. Pressure calibrations were obtained in situ, within the shock-tunnel flow, during the experimental program.

### A. Shear Calibration

Shear calibrations were performed by monitoring the skin-friction transducer output following the sudden release of a known shear load. The gauge was supported in a cast iron block using the mounting system of Fig. 2. As shown in Fig. 3a, the block was oriented so that the gauge sensing disk was in the vertical plane, with the sensing axis horizontal. A cotton thread arrangement was then directly adhered, along the center of the sensing disk, using cyanoacrylate glue. The thread was approximately 0.2 mm in diameter. This arrangement, with a weight of known mass $m$, then produced an effective static shear stress, aligned with the sensing axis, according to

$$\tau_w = \frac{4mg}{\pi D^2 \tan(\theta)} \tag{1}$$

Here $\tau_w$ is based on the force applied through thread A divided by the area of the sensing disk, $\theta$ is the angle between the horizon and thread C, $g$ is the acceleration of gravity, and $D$ is the diameter of the sensing disk. The load on the gauge was then impulsively released by striking the weight from below with a hard metal object. Shown in Fig. 3b, the output from the measuring piezoceramic, $V_1$, typically had a 10–90% rise time near 1 ms. This relatively long rise time was confirmed to be an elasticity-induced trait of the cotton thread arrangement and not a function of the skin-friction gauge rise time. In the confirmation test, thread A was adhered to the center of the sensing diaphragm of a PCB™-type piezoelectric pressure transducer. The thread and transducer were arranged such that the sensing diaphragm plane was perpendicular to the applied force. The gauge had a manufacturer specified rise time of 2 $\mu$s. The pressure transducer output, resulting from load release, was found to have a rise time near 1.3 ms and was similar in shape to that of the skin-friction gauge.

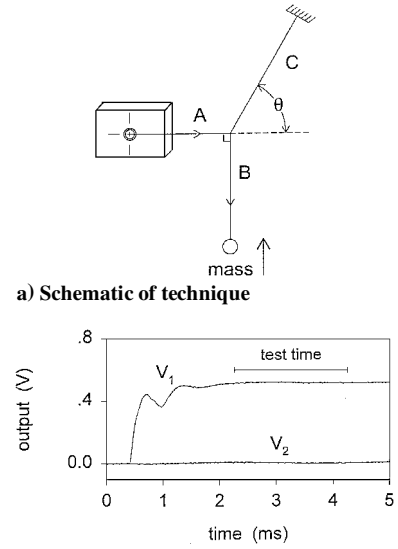


a) Schematic of technique

b) Example of time-resolved gauge output

**Fig. 3 Skin-friction transducer shear calibration.**

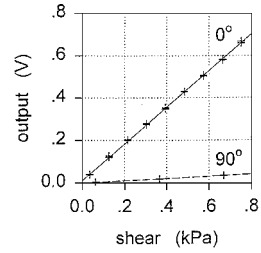


**Fig. 4 Shear calibration example.**

Sensitivity of the skin-friction transducer to a given shear load was established by determining the average level of the measuring element output $V_1$ over a given test time (as shown in Fig. 3b). To minimize errors introduced because of the charge amplifier decay time constant, the test time was chosen to resemble the shock-tunnel test time in terms of duration and time from load application. As is evident in Fig. 3b, the acceleration piezoceramic response, $V_2$, was negligible during the calibration tests.

Calibrations were performed over a skin-friction range of 0–800 Pa and 0–4000 Pa. Gauge output was found to be very linear because the maximum deviation of the calibration points, from a zero-based best straight line, was less than 1.5% of full scale. A typical calibration and resulting linear regression are presented in Fig. 4. The coefficient of determination (correlation coefficient squared) was typically near 0.9998; indicating a highly significant linear correlation. Deviation of the regression line from the origin was neglected during subsequent gauge use, and this represented an error of 1% or less for typical operating levels. For each of the calibration ranges, the calibration was checked by repeating the procedure with the gauge rotated by 180 deg. Typical agreement for the calibration slope was near 1% for the two orientations. The average slope or shear sensitivity, $d$, was typically near $0.8 \times 10^{-3}$ V/Pa, and individual gauge calibrations were found to be very stable with age.

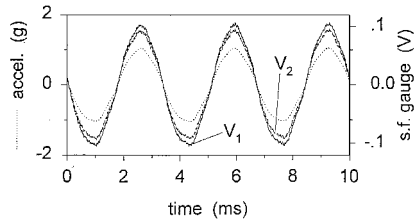


**Fig. 5 Example of skin-friction transducer output (measuring, $V_1$, and acceleration, $V_2$, elements) and reference accelerometer output during acceleration calibration.**

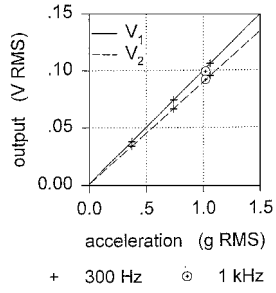


**Fig. 6 Acceleration calibration example.**

The total experimental uncertainty in $d$ was established to be near $\pm 1\%$. This followed consideration of the random error introduced by the calibration method and systematic errors of establishing the mass of the calibration weights, the angle of thread C, and the diameter of the sensing disk. The systematic errors introduced through data recording and through possible misalignment between the sensing axis of the transducer and the calibration force applied through thread A were also considered.

Cross axis sensitivity, at 90- and 270-deg orientation, was explored for the 0–800-Pa calibration range. Sensitivity to transverse shear was typically near 6% of the measuring axis sensitivity. An example linear regression of cross axis calibration data is presented in Fig. 4.

### B. Acceleration Calibration

Acceleration calibrations were performed by vibrationally exciting the gauge, along the sensing axis, using an electrodynamic vibrator. The gauge was mounted rigidly to the vibrator drive spindle, and a reference accelerometer was mounted on the spindle centerline.

A nominal excitation frequency of 300 Hz was used for the calibrations. This frequency approximately matched the dominant frequency of acceleration experienced by gauges during early prototype testing in the shock tunnel. A check measurement at 1 kHz was also obtained, and it was established that the effect of altering excitation frequency was small. Figure 5 presents typical outputs of the measuring, $V_1$, and the acceleration, $V_2$, elements of the skin-friction gauge and the accelerometer during electrodynamic vibrator operation. The three signals can be seen to be in phase. A typical linear regression of gauge rms output against accelerometer rms output is presented in Fig. 6. Ascertainment of the ratio of measuring element output to acceleration element output allowed for routine subtraction of the acceleration component of the measuring element signal during service. The mean acceleration calibration constant $c = (V_1 \text{ rms}/V_2 \text{ rms})_{\text{mean}}$ was typically 1.1.

An uncertainty analysis of the calibration method indicated that the constant $c$ could be determined to within $\pm 3\%$. This estimate was based on a root square sum of the systematic uncertainty of data recording and a 95% confidence interval for the uncertainty of the mean of four calibration points.

### C. Pressure Calibration

Pressure calibrations were obtained through a series of paired runs, in the shock tunnel, during the experimental program. The technique was found to produce more reliable and repeatable results than other bench top methods trialed by Kelly.[15] For the present technique, measurements were obtained for one condition in the impulse facility and then repeated with the skin-friction transducer rotated by 180 deg relative to the test flow. The shear component of the gauge output, $V_{sf}$, changed sign once rotated; however, the pressure component, $V_P$, did not. When the mean of the two signals was compared with the average static pressure measured adjacent to the transducer, the pressure sensitivity of the transducer was established. This technique is represented by

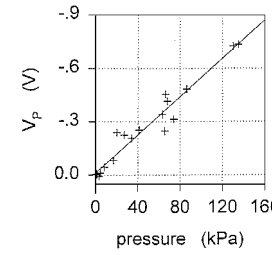


**Fig. 7 Pressure calibration example.**

$$V_P = (V_0 + V_{180})/2 \tag{2}$$

where $V_0 = +V_{sf} + V_P$ and $V_{180} = -V_{sf} + V_P$. Here $V_0$ and $V_{180}$ are the acceleration compensated outputs of the skin-friction gauge for the two orientations. Calibration runs were conducted in the shock tunnel using the same test models that were used for the experimental program.[5,6]

An example of a linear regression of $V_P$ as a function of the mean measured static pressure is presented in Fig. 7. Even though the data were obtained for a broad range of flow conditions, the correlation with average pressure is found to be highly significant. The data represent tests with laminar and turbulent boundary layers,[6] over a range of stagnation enthalpies, and tests with and without hydrogen combustion in the freestream.[5] Linear regressions, in the form of $V_P = bP + e$, were performed over a low- and high-pressure range for each skin-friction transducer. In general, the correlations were found to be significant. Absolute values of the pressure calibration constants, $b$ and $e$, were typically $4 \times 10^{-3}$ V/kPa and $10 \times 10^{-3}$ V, respectively.

An uncertainty analysis for the pressure calibration technique was performed.[6] The analysis accounted for factors such as systematic uncertainties in pressure measurement and data recording, repeatability of static pressure and skin-friction levels between pairs of calibration tests, and overall random error introduced by the technique. It was established that the total uncertainty in the constants $b$ and $e$ was approximately $\pm 80$ and $\pm 500\%$, respectively. Such large uncertainty levels resulted from large random errors and reflected an inherent randomness of the calibration technique and a lack of comprehensive calibration data for some gauges. However, for the flow conditions of the experiments of Refs. 5 and 6, the pressure component of the transducer signal, $V_p$, was typically 10 and 30%, respectively, of the shear component, $V_{sf}$. Therefore, as discussed later, the resulting levels of total uncertainty in measured skin friction were acceptable, particularly for high-Reynolds-number measurements.

### D. Natural Frequency Determination

To circumvent a complex theoretical analysis, an empirical technique was devised to assess the resonant behavior of the skin-friction transducer. The technique provided an impulse input to the skin-friction gauge sensing disk and, hence, excited a state of free damped vibration. The method involved rolling a 4-mm-diam, stainless-steel ball bearing off a 25-deg ramp and onto the sensing disk. The ramp was aligned with the transducer measuring axis, and the gauge was supported in a cast iron block using the mounting system of Fig. 2. The ball obliquely struck the disk on the measuring axis; however, the impact point was away from the gauge axial center. This arrangement was aimed at simultaneously exciting shear, translational, and rotational modes of vibration. The ball bounced off the face of the gauge and did not strike the transducer a second time. The output from the gauge measuring element indicated an impulse of approximately 40 $\mu$s in duration was applied. Fast Fourier transforms were performed on the measuring and acceleration element outputs to determine the spectral response of the gauge. In general, three to four dominant resonant frequencies were identified for both the measuring and acceleration elements. For the group of transducers tested, resonant frequencies were in the range of 30–60 kHz. The group

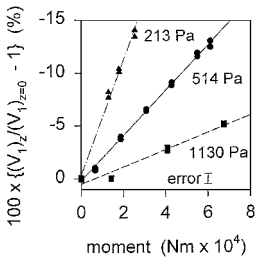


**Fig. 8 Example of skin-friction transducer sensitivity to moments on sensing disk; sensitivity presented for effective skin-friction loads of 213, 514, and 1130 Pa.**

average of lowest gauge natural frequency was found to be near 40 kHz.

### E. Moment Sensitivity

An off-center axial force on the sensing invar disk will result in a moment being applied to the measuring piezoceramic. Such a force will be applied if the skin-friction transducer is operated in a flow with a pressure gradient. Piezoceramics operated in shear mode are inherently insensitive to moments, however, a technique was devised to quantify the effect.

A moment was applied to the sensing disk using a 16-mm-long, 2-mm-diam brass post that had a 10-mm-diam flange on one end. The flange was adhered to the sensing disk of the skin-friction transducer using double-sided adhesive tape. The gauge was then mounted in a prone position within a cast iron block using the mount in Fig. 2. The sensing axis of the gauge was aligned such that it was vertical, and calibration weights were hung from the post using a cotton thread. In a manner similar to the shear calibration tests, the load was then impulsively released. In contrast to the shear tests, however, the load was equivalent to a simultaneous moment and shear force. The levels of applied moment and shear were adjusted by using different calibration weights and locating the thread at differing distances along the post. The measuring element output was temporally similar to that of the shear calibrations. However, the level of output was only repeatable to within ±25%; hence, the results of this technique are regarded as an approximate guide. The output from the acceleration element was approximately 5% of the measuring element output and was neglected.

An example of the relationship between the measuring element output and applied moment and shear is presented in Fig. 8. The level of applied moment was determined as a product of the force due to gravity of the calibration weight and the distance of the cotton thread from the gauge sensing disk, $z$. The output from the measuring element was normalized with respect to the corresponding output for the same shear load but with zero moment. Unity was then subtracted from this ratio, and the result is presented in Fig. 8 as a percentage. The vertical scale of the graph, hence, represents the systematic error that would be introduced if the gauge is assumed to have zero sensitivity to moments and yet is operated in an environment that introduces one. Three different calibration weights were used, and each effective wall shear stress is indicated in Fig. 8. Interestingly, it can be seen that the measuring element is more sensitive to an applied moment when the simultaneous level of applied shear is low.

At this point, it is important to quantify the level of moment that is applied to the sensing disk for a given pressure gradient. If a pressure gradient of $\mathrm{d}P/\mathrm{d}x$ (kPa/m) is applied across the sensing disk, it can be shown by integrating the pressure across the face that the moment $J$ about the centerline of the disk is given by

$$J = \frac{\mathrm{d}P}{\mathrm{d}x}\frac{\pi D^4}{0.064} \tag{3}$$

Hence, if a positive pressure gradient is exerted across the transducer face, a positive moment will result on the sensing disk, and based on Fig. 8, the skin-friction gauge will underpredict. For example, maximum observed pressure gradients in the scramjet combustor of Ref. 5 were near 800 kPa/m, and from Eq. (3), this is equivalent to a moment of $4 \times 10^{-4}$ N·m. When it is considered that measured skin-friction levels were typically greater than 1000 Pa, Fig. 8 indicates that if moment sensitivity is neglected, then a bias of less than 3% is introduced into the measurements. Therefore, as expected, the response of the transducer piezoceramic to induced moment is negligible, and hence, the effect is omitted from the calibration summary equations that follow. The resulting bias of this omission, however, is incorporated into the systematic uncertainty of the experimental measurements of skin friction.

### F. Calibration Summary

The established calibration constants can now be combined to determine the in-service skin friction acting on the transducer during the experimental measurements. The output of the exposed measuring element $V_1$ can be represented by

$$V_1 = V_{\mathrm{sf}} + V_P + V_{a,1} \tag{4}$$

where $V_{\mathrm{sf}}$, $V_P$, and $V_{a,1}$ are the components of voltage output due to shear, static pressure, and experienced acceleration, respectively. The output of the protected acceleration element $V_2$ can be represented by

$$V_2 = V_{a,2} \tag{5}$$

where $V_{a,2}$ is the voltage output due to experienced acceleration. Because the element is not exposed to the flow, the shear and pressure components of the signal are equal to zero.

The calibration techniques have established the following: 1) acceleration, $V_{a,1} = cV_{a,2}$; 2) shear, $V_{\mathrm{sf}} = d\tau_w$; and 3) pressure, $V_P = bP + e$.

Combining these linear relationships with Eqs. (4) and (5) reveals the skin friction acting on the sensing disk of the gauge is given by

$$\tau_w = [V_1 - cV_2 - (bP + e)]/d \tag{6}$$

Before estimates of the total uncertainty in determined $\tau_w$ were made, consideration was given to errors introduced through transducer design and operation. According to the work of others,[13,19] sensing disk protrusion and gap flow disturbances to the boundary layer will be minimal for the transducer dimensions and boundary-layer conditions of interest. If the transducer is to be operated in a pressure gradient, consideration must be given to gap flow and to forces induced on the measuring element because of unequal pressure around the edge of the sensing disk.[13] As discussed earlier, moment sensitivity must also be considered. Following further consideration of the uncertainty of the quantities in the right-hand side of Eq. (6), that is, uncertainty in the calibration constants and in pressure and voltage measurement, the total experimental uncertainty in measured skin friction was determined.[6] The total uncertainty is dependent on test flow conditions and skin-friction levels. However, for an experiment of Ref. 6, $\tau_w$ could typically be measured to within ±47% for a laminar boundary layer, to within ±16% for a transitional boundary layer, and to within ±7% for a turbulent boundary layer. Whereas, for the scramjet combustor experiment of Ref. 5, $\tau_w$ could typically be measured to within ±12%.

Table 1 provides a summary of the established characteristics of a typical skin-friction transducer.

## Measurements

The experiments were performed in the T4 free piston shock tunnel at the University of Queensland. The measurements reported here were obtained on a 1.5-m-long flat plate that formed one of the inner walls of a rectangular duct. The duct had a 120 × 60 mm inlet, which captured air issuing from the 260-mm-diam exit of the facility's hypersonic nozzle. Skin-friction transducers, thin-film heat flux gauges, and pressure transducers were mounted at a series of locations that extended axially along the instrumented plate. Measurements in laminar, transitional, and turbulent boundary layers were obtained. The experiment, results, and analysis are fully discussed in Ref. 6.

A time-resolved skin-friction transducer output for a laminar boundary-layer measurement is presented in Fig. 9. Figure 9a shows the raw output from the measuring and acceleration elements, $V_1$ and $V_2$, respectively. The highly underdamped, high-frequency resonant behavior of the transducer is clearly evident. A 30-$\mu$s moving time average of the gauge output is presented in Fig. 9b. The measuring element signal shows a sudden positive increase following test gas

**Table 1 Specification summary for a typical skin-friction transducer**

| Specification | Value |
|---|---|
| Maximum calibrated range | 0–4,000 Pa |
| Resolution (with 30-$\mu$s time average) | 1 Pa |
| Sensitivity (nominal at 296 K) | $0.8 \times 10^{-3}$ V/Pa |
| Linearity (zero-based best straight line) | 1.5% FS |
| Cross axis shear sensitivity | 6% |
| Pressure sensitivity | $4 \times 10^{-3}$ V/kPa |
| Lowest resonant frequency | ~40 kHz |
| Frequency range ±5% | 20–10,000 Hz |
| (approximate) ±10% | 15–12,000 Hz |
| Decay time constant | 47 ms |
| Polarity (at 0 deg) | Positive |
| Maximum operating temperature | 380 K |
| Temperature sensitivity | ~0.5%/K |
| Maximum heat flux over 3 ms | 7.5 MW/m$^2$ |
| Maximum static pressure | ~14 MPa |
| Sensing element diameter | 10 mm |
| Element to housing gap (nominal) | 0.16 mm |
| Piezoceramic material | PZT-5H |
| Sensing element material | Invar |
| Housing material | Brass |
| Total weight | $98 \times 10^{-3}$ kg |
| Excitation (constant current) | 4 mA |
| Voltage to current regulator | 12–24 V dc |
| Connector | B&K$^{TM}$ microdot × 2 |

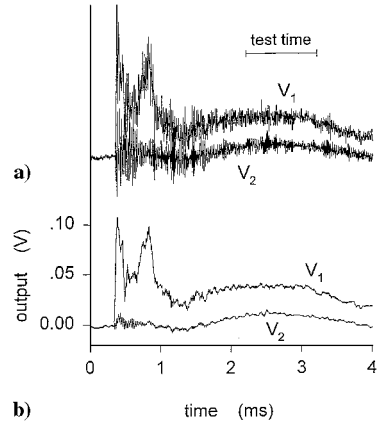


**Fig. 9 Skin-friction transducer in laminar boundary layer: a) raw output and b) output with 30-$\mu$s moving time average.**

arrival and subsequent fluctuations during the flow establishment processes of the duct and facility (up to 1.2 ms). Indications that the gauge experienced vibration with a frequency near 200 Hz then follows. This is confirmed by the acceleration element output. During the indicated test time, the acceleration signal represented approximately 30% of the measuring element signal. In general, the average level for laminar testing was 12%. This compares with later higher shear stress turbulent measurements in which the acceleration signal was generally 8% of the measurement element signal.

From knowledge of the static pressure history adjacent to the transducer, Eq. (6) can be used to obtain the temporal variation in measured skin friction. This is presented in Fig. 10, together with the static pressure history. It can be seen that the skin friction is relatively steady during the designated test time and confirms that sufficient time was allowed for flow and boundary-layer establishment in the determination of the test time. To within experimental uncertainty, the level of test time skin friction is in agreement with steady laminar theory.[20] The high level of experimental uncertainty in the measurement reflects the combination of low wall shear stress of the laminar boundary layer and a large error introduced by the gauge pressure calibration technique.

Figure 11 presents the temporal variation in measured skin friction and static pressure for a turbulent boundary layer. Again, flow establishment processes result in fluctuations of the boundary-layer skin friction before the onset of the test time. The test time level of

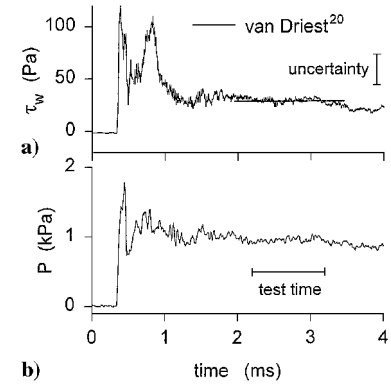


**Fig. 10 Laminar boundary-layer measurements with 30-$\mu$s moving time average, $Re_x = (2.5 \pm 0.4) \times 10^5$: a) skin-friction record and b) static pressure record.**

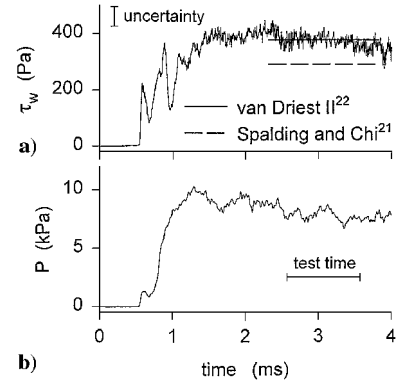


**Fig. 11 Turbulent boundary-layer measurements with 30-$\mu$s moving time average, $Re_x = (6.7 \pm 1) \times 10^6$: a) skin-friction record and b) static pressure record.**

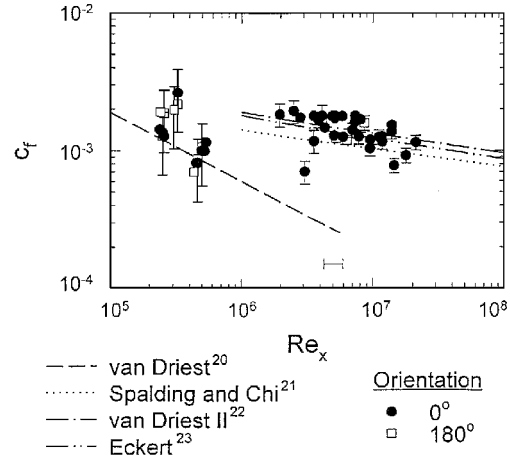


**Fig. 12 Measured axial distribution of skin-friction coefficient and comparison with theory, $M \approx 6.6$, $h_s \approx 3.5$ MJ/kg (Mach 8 simulated flight speed) and $h_w = 0.3$ MJ/kg (representative error bars displayed).**

measured skin friction is compared with two popular correlations for steady turbulent boundary layers.[21,22]

For each of the preceding examples, the skin-friction coefficient was determined using estimated flow conditions and the mean level of skin friction during the test time. The results are plotted in Fig. 12 as a function of Reynolds number, together with other data obtained for a series of tests with similar flow Mach number and stagnation enthalpy. The data are identified in Fig. 12 in terms of the skin-friction transducer orientation to the test flow. Absolute values of skin-friction coefficient are displayed for the 180 deg measurements and the general agreement of these levels with the 0 deg data provides evidence of correct operation of the skin-friction

transducer. The magnitude of scatter in measured skin-friction coefficient was of the same order as in measured Stanton number.[6]

Theoretical laminar[20] and turbulent[21–23] predictions are also presented in Fig. 12. It can be seen that there is generally good accord between theory and experiment. However, the high-Reynolds-number data do not agree with one turbulent boundary-layer correlation. Reference 6 identified a strong unit-Reynolds-number trend in the difference between experiment and theory for these data and for other data at different stagnation enthalpies and Mach numbers. It was established that the correlations of van Driest[22] and Eckert[23] were in better agreement with the data at low unit Reynolds numbers. However, the Spalding and Chi[21] correlation performed better at high unit Reynolds numbers. The unit-Reynolds-number trend was attributed to nonequilibrium turbulent boundary-layer flow at low unit Reynolds numbers, even though the measurements were obtained well downstream of a transition region defined using the heat flux data. The trend is somewhat reflected in the Reynolds number plot of Fig. 12. The results are discussed further in Ref. 6.

## Conclusions

The design, calibration, and operation of a new acceleration compensated piezoelectric skin-friction transducer have been reported. The gauge is particularly suited to use in hypervelocity impulse facilities because its lowest natural frequency is near 40 kHz.

The transducer design incorporated a measuring element that was exposed to the test flow and an acceleration element that was mounted internally. Each element contained a piezoceramic that was operated in shear mode, and the ceramic's anisotropic characteristics enabled pressure, transverse shear, and moments to be decoupled effectively from the skin-friction shear force. Thermal insulation, heat conduction control, electrical shielding, and vibration isolation were also important features of the new gauge design and mounting configuration.

The skin-friction transducer was calibrated for shear, acceleration, and moment inducing forces in separate bench tests. For these calibration tests, linear correlations between input and response were highly significant. The shear calibrations exhibited this level of linearity over a wide operating range, (0–4000-Pa wall shear stress). Pressure calibrations were performed in situ, during the experimental program. For this technique, regressions of the results typically exhibited a significant linear correlation.

Uncertainty analyses were conducted for the calibration, compensation, and measurement methods. The inherent uncertainty in the pressure calibration technique introduced a large systematic relative error in skin-friction measurements for operating conditions typical of laminar boundary layers. It was established, however, that for more complex, less understood flows such as turbulent boundary layers and scramjet combustion fields, skin friction could be measured to within a typical uncertainty of $\pm 7$ to 12%.

Sample measurements from a shock tunnel were presented, and the results demonstrated reliable operation of the skin-friction gauge. The successful development of the new transducer has allowed further exploration of viscous drag levels encountered in hypersonic flight. Further investigation to reduce experimental errors, in particular, will allow an even greater insight.

## Acknowledgments

The authors are thankful for the financial support provided by the Australian Research Council for operation of the T4 shock tunnel and for the financial support of NASA Langley Research Center, through NASA Grant NAGW-674, during early stages of the project. The authors are appreciative of the technical assistance provided by J. Brennan and B. Allsop in the development of the skin-friction transducers.

## References

[1] Erdos, J. I., "Scramjet Testing in Shock-Heated Tunnels," *Proceedings of the 21st International Symposium on Shock Waves* [CD-ROM], edited by A. F. P. Houwing, Australian National Univ., Canberra, Australia, 1997.

[2] Wright, C. P., *Applied Measurement Engineering*, Prentice–Hall, London, 1995, pp. 74, 155, 156.

[3] Simmons, J. M., "Measurement Techniques in High Enthalpy Hypersonic Facilities," *Experimental Heat Transfer, Fluid Mechanics and Thermodynamics*, edited by M. D. Kelleher, K. R. Sreenivasan, R. K. Shah, and Y. Joshi, Vol. 1, Elsevier Science, Amsterdam, 1993, pp. 43–60.

[4] Jessen, C., and Gronig, H., "A Six Component Balance for Short Duration Hypersonic Facilities," *New Trends in Instrumentation for Hypersonic Research*, edited by A. Boutier, Kluwer, Dordrecht, The Netherlands, 1993, pp. 295–305.

[5] Goyne, C. P., Stalker, R. J., and Paull, A., "Shock-Tunnel Skin-Friction Measurement in a Supersonic Combustor," *Journal of Propulsion and Power*, Vol. 15, No. 5, 1999, pp. 699–705.

[6] Goyne, C. P., "Skin Friction Measurements in High Enthalpy Flows at High Mach Number," Ph.D. Dissertation, Dept. of Mechanical Engineering, Univ. of Queensland, Brisbane, Queensland, Australia, 1998.

[7] Wallace, J. E., "Hypersonic Turbulent Boundary-Layer Studies at Cold Wall Conditions," Heat Transfer and Fluid Mechanics Inst., 1967, pp. 427–451; also NASA CR-82425.

[8] Holden, M. S., "An Experimental Investigation of Turbulent Boundary Layers at High Mach Number and Reynolds Numbers," NASA CR-112147, 1972.

[9] Holden, M. S., "Ground Test Facilities and Instrumentation for Aerothermal and Aero-Optical Studies of Hypersonic Interceptors," *New Trends in Instrumentation for Hypersonic Research*, edited by A. Boutier, Kluwer, Dordrecht, The Netherlands, 1993, pp. 65–74.

[10] Jessen, C., Vetter, M., and Gronig, H., "Experimental Studies in the Aachen Hypersonic Shock Tunnel," *Zeitschrift für Flugwissenschaften und Weltraumforschung*, Vol. 17, April 1993, pp. 73–81.

[11] Bowersox, R. D. W., Schetz, J. A., Chadwick, K., and Deiwert, S., "Technique for Direct Measurement of Skin Friction in High Enthalpy Impulsive Scramjet Flowfields," *AIAA Journal*, Vol. 33, No. 7, 1995, pp. 1286–1291.

[12] Novean, M. G., Schetz, J. A., and Bowersox, R. D. W., "Direct Measurements of Skin Friction in Complex Supersonic Flows," AIAA Paper 97-0394, 1997.

[13] Winter, K. G., "An Outline of the Techniques Available for the Measurement of Skin-Friction in Turbulent Boundary Layers," *Progress in Aerospace Sciences*, Vol. 18, No. 1, 1977, pp. 1–57.

[14] Kelly, G. M., Simmons, J. M., and Paull, A., "Skin-friction Gauge for Use in Hypervelocity Impulse Facilities," *AIAA Journal*, Vol. 30, No. 3, 1992, pp. 844, 845.

[15] Kelly, G. M., "A Study of Reynolds Analogy in a Hypersonic Boundary Layer Using a New Skin Friction Gauge," Ph.D. Dissertation, Dept. of Mechanical Engineering, University of Queensland, Brisbane, Australia, 1994.

[16] Jaffe, B., Cook, W. R., and Jaffe, H., *Piezoelectric Ceramics*, Academic Press, London, 1971, pp. 1–21.

[17] Bies, D. A., and Hanson, C. H., *Engineering Noise Control*, Unwin Hyman, London, 1988, pp. 299–303.

[18] White, F. M., *Viscous Fluid Flow*, 2nd ed., McGraw–Hill, New York, 1991, pp. 435, 436.

[19] Allen, J. M., "Improved Sensing Element for Skin-Friction Balance Measurements," *AIAA Journal*, Vol. 18, No. 11,1980, pp. 1342–1345.

[20] van Driest, E. R., "Investigation of Laminar Boundary layer in Compressible Fluids Using the Crocco Method," NACA TN 2597, 1952.

[21] Spalding, D. B., and Chi, S. W., "The Drag of a Compressible Turbulent Boundary Layer on a Smooth Flat Plate with and Without Heat Transfer," *Journal of Fluid Mechanics*, Vol. 18, 1964, pp. 117–143.

[22] van Driest, E. R., "The Problem of Aerodynamic Heating," *Aeronautical Engineering Review*, Vol. 15, No. 10, 1956, pp. 26–41.

[23] Eckert, E. R. G., "Engineering Relations for Friction and Heat Transfer to Surfaces in High Velocity Flow," *Journal of the Aeronautical Sciences*, Vol. 22, 1955, pp. 585–587.

R. P. Lucht
*Associate Editor*